sciendo

Polish Journal of Chemical Technology, 26, 1, 102—112, 10.2478/pjct-2024-0016

Synthesis, characterization, and molecular modeling of novel 1,3,4-oxadiazole derivatives of mefenamic acid

Mashooq A. Bhat*, Ahmed M. Naglah, Ahmed Hassan Bakheit, Mohamad A. Al-Omar

Department of Pharmaceutical Chemistry, College of Pharmacy, King Saud University, Riyadh 11451, Saudi Arabia
Corresponding author: e-mail: mabhat@ksu.edu.sa

A novel series of 1,3,4-oxadiazole derivatives of mefenamic acid was obtained by reacting hydrazones of mefenamic acid with anhydrous acetic anhydride. The mefenamic hydrazones were obtained by reacting different substituted aldehydes with mefenamic acid hydrazide. All the compounds were characterized by spectral data and elemental analysis. Molecular docking studies of all the compounds were performed against COX-1/COX-2 enzymes. Compound **4** and compound **10** were found to have the highest potential to bind with COX-1 while compound **3**, compound **6**, and compound **10** were found to have the highest potential to bind with COX-2 enzyme.

Keywords: Mefenamic acid; 1,3,4-Oxadiazoles, Hydrazones, Molecular docking; COX-1/COX-2 enzymes.

INTRODUCTION

Fenamates are non-steroidal anti-inflammatory drugs (NSAIDs) used as potent analgesic and anti-inflammatory agents in the treatment of osteoarthritis, rheumatoid arthritis, and other painful musculoskeletal illnesses[1–4]. The fenamates exhibit pharmacologic actions similar to those of aspirin. They are potent inhibitors of cyclooxygenase, thereby inhibiting the release of prostaglandins[5]. Mefenamic acid is a well-known nonsteroidal anti-inflammatory drug. In the literature, *N*-arylhydrazone derivatives of mefenamic acid were synthesized and evaluated for analgesic and anti-inflammatory activity. The results concluded that replacing the acidic moiety of mefenamic acid with *N*-arylhydrazone moiety can create potent analgesic anti-inflammatory compounds[6]. 1,3,4-Oxadiazole derivatives of mefenamic acid were synthesized and evaluated for analgesic and anti-inflammatory activity. The oxadiazole ring being weak and acidic in nature reduces the ulcerogenicity of mefenamic acid and retains its anti-inflammatory potential[7]. However, 1,3,4-oxadiazole is more important because of its remarkable biological activities. Compounds containing 1,3,4-oxadiazole structure possess various pharmacological effects including antibacterial, antifungal, antitubercular, anticonvulsant, anti-allergic, anti-inflammatory, cytotoxic, and insecticidal activities[8–21]. This structure can be used as a bioisoester for carboxylic acids, esters, and carboxamides. Derivatives of oxadiazole such as tiodazosin, nosapidil, and furamizole have been introduced as antihypertensive and antibacterial agents, respectively.

In drug discovery research, molecular docking is a widely used computational technique that simulates the interaction between a ligand and a target molecule in a biological system. It can help to screen and rank compounds based on their binding affinity and specificity by using energy calculations and conformational sampling[22]. It can also provide insights into the molecular mechanisms of ligand-target recognition[23, 24]. ADMET testing, which is another essential technique in drug discovery research that evaluates the physicochemical properties of a compound under physiological conditions. It can also help to assess the safety and efficacy of a compound for further development by measuring how a compound is absorbed, distributed, metabolized, excreted, and toxic in the human body after administration[25].

In the present study, we investigated the COX-1/COX-2 inhibitor activity of novel 1,3,4-oxadiazole derivatives **(1–12)**, derived from mefenamic acid. Our main objective was to identify the most potent synthesized compound among them by molecular modelling. We also analyzed the drug likeness and ADMET profile of the compounds to determine their suitability for further drug development. By combining molecular docking and ADMET testing, we aimed to discover novel and effective drug candidates.

EXPERIMENTAL

Chemistry

Thin layer chromatography (TLC) was performed on Silica gel $60F_{254}$ (Merck). Perkin Elmer FT-IR spectrophotometer was used for IR spectroscopy. Gallenkamp melting point apparatus was used for melting point determination. ^{1}H NMR spectrum of the compounds was performed on Bruker NMR 700 MHz and ^{13}C NMR spectrum of the compounds was performed on Bruker NMR 176 MHz. Mass spectra of the compounds were performed on Agilent triple quadrupole 6410 TQ GC/MS equipped with ESI (electrospray ionization). Following chemicals with CAS numbers were purchased from chemical companies for the synthesis of target compounds. Mefenamic acid (CAS no. 61687, Sigma Aldrich), Sulfuric acid (CAS no. 7664939, Merck), ethyl acetate (CAS no. 141786, Merck), Hydrazine hydrate (CAS no. 10217-52-4, Sigma Aldrich), ethanol (CAS no. 64175, Merck), Glacial acetic acid (CAS no. 64197), anhydrous acetic anhydride (CAS no. 108247, Merck).

*Preparation of methyl 2-(2,3-dimethylanilino) benzoate **(ii)***

To a solution of mefenamic acid (5.0 g, 0.02 mol) in MeOH (15 mL), conc. H_2SO_4 (1.5 mL) was added carefully. The solution was refluxed for 18 h and the progress of the reaction was monitored by TLC. After completion of the reaction, the solvent was evaporated. The crude was added to water, neutralized by NaOH (2 mol), until pH was 7.0, and finally extracted with ethyl acetate (3 × 25 mL). The combined ethyl acetate layer was washed with brine, dried over anhydrous Na_2SO_4 and concentrated under reduced pressure. The residue obtained was purified by column chromatography on a silica gel column to afford the desired product as

a white solid (4.1 g, 80% yield); M. p. 96–98 °C, ^{1}H NMR (DMSO-d_6, 700 MHz) δ (ppm): 2.10 (3H, s, CH_3), 2.29 (3H, s, CH_3), 3.87 (3H, s, OCH_3), 6.67–6.73 (2H, m Ar-H), 7.05 (1H, d, J = 7 Hz, Ar-H), 7.13 (2H, t, J = 7 Hz, Ar-H), 7.33 (1H, t, J = 7 Hz, Ar-H), 7.88 (1H, d, J = 14 Hz, Ar-H), 9.19 (1H, s, NH, D_2O Exchg.), ^{13}C NMR (176 MHz, DMSO-d_6) δ (ppm): 14.1 (CH_3), 20.6 (CH_3), 52.3 (OCH_3), 110.8, 113.7, 116.9, 123.0, 126.5, 127.1, 131.6, 132.0, 135.0, 138.6, 149.0, 168.8.

*Preparation of 2-(2,3-dimethylphenylamino) benzohydrazide **(iii)***

To a solution of mefenamic methyl ester (1 g, 0.004 mol) in EtOH (10 mL), hydrazine hydrate (2 mL) was added dropwise and the solution was stirred. The temperature of the mixture was raised gradually to 95–100 °C and was maintained for 12 h. The reaction mixture was then concentrated under reduced pressure and the residue was diluted with water (10 mL). The aqueous layer was extracted with chloroform (3 × 25 mL). The organic layers were collected, combined, washed with brine (10 mL), dried over anhydrous Na_2SO_4 and concentrated under reduced pressure. The solid obtained was purified by crystallization from EtOH, filtered and dried to give the desired compound as a yellow solid (0.82 g, 80% yield); m. p.: 118–120 °C.; ^{1}H NMR (DMSO-d_6, 300 MHz) δ (ppm): 2.09 (s, 3H), 2.26 (s, 3H), 6.67 (d, J = 4 Hz, 1H), 6.67–7.03 (m, 3H), 7.10–7.25 (m, 2H), 7.30–7.40 (m, 1H), 7.65–7.68 (m, 1H), 9.0 (s, 1H), 9.40 (s, 1H), 9.80 (s, 1H), 10.51 (s, 1H); MS m/z 256 (M+, 100%)[32].

*General synthesis of final compounds **(1–6)***

A solution of the mefenamic hydrazide (2.56 g, 0.01 mol) and substituted aldehyde (0.011 mol) in ethanol (15 mL) with catalytic amount of glacial acetic acid was refluxed for three hours. The progress of the reaction was monitored by TLC. After completion, the reaction mixture was diluted by using ice cold water (25 mL) with stirring. The solid separated was filtered, washed with ice cold water and recrystallized from EtOH to afford the expected product.

2-(2,3-Dimethylanilino)-N'-[(E)-(2,4,5-trimethoxyphenyl) methylidene] benzohydrazide **(1).**

Yield: 80%; m. p.: 240–242 °C; FT-IR (KBr) ν cm^{-1}: 2987 (NH str.), 1588 (C=O), 1507 (C=N), 1269 (C-O); ^{1}H NMR (700 MHz, DMSO-d_6) δ (ppm): 2.13 (3H, s, CH_3), 2.29 (3H, s, CH_3), 3.77 (3H, s, OCH_3), 3.87 (6H, d, J = 7 Hz, 2×OCH_3), 6.78 (2H, m, Ar-H), 6.85 (1H, d, J = 14 Hz, Ar-H), 6.95 (1H, d, J = 5.6 Hz, Ar-H), 7.08 (2H, d, J = 14 Hz, Ar-H), 7.29 (1H, t, J = 7 Hz, Ar-H), 7.37 (1H, s, Ar-H), 7.75 (1H, d, J = 7 Hz, Ar-H), 8.73 (1H, s, =CH), 9.31 (1H, s, NH, D_2O exchg.), 11.76 (1H, s, CONH, D_2O exchg.); ^{13}C NMR (176 MHz, DMSO-d_6) δ (ppm): 14.1, 20.7, 56.2, 57.0, 98.3, 108.0, 114.4, 116.5, 117.2, 120.5, 125.7, 126.3, 129.3, 130.0, 132.8, 138.2, 139.5, 143.7, 144.0, 147.0, 152.5, 153.8, 165.5; MS: m/z = 433.49 [M]$^+$; $C_{25}H_{27}N_3O_4$.

2-(2,3-Dimethylanilino)-N'-[(E)-(3,4,5-trimethoxyphenyl) methylidene] benzohydrazide **(2)**

Yield: 80%; m. p.: 230–232 °C; FT-IR (KBr) ν cm^{-1}: 3013 (NH str.), 1630 (C=O), 1508 (C=N), 1320 (C-O); ^{1}H NMR (700 MHz, DMSO-d_6) δ (ppm): 2.13 (3H, s, CH_3), 2.29 (3H, s, CH_3), 3.72 (3H, s, OCH_3), 3.85 (6H, s, 2×OCH_3), 6.81 (1H, t, J = 7 Hz, Ar-H), 6.85 (1H, d, J = 7 Hz, Ar-H), 6.95 (1H, d, J = 7 Hz, Ar-H), 7.03 (2H, s, Ar-H), 7.09 (2H, d, J = 7 Hz, Ar-H), 7.31 (1H, t, J = 7 Hz, Ar-H), 7.73 (1H, d, J = 7 Hz, Ar-H), 8.36 (1H, s, =CH), 9.21 (1H, s, NH, D_2O exchg.), 11.89 (1H, s, CONH, D_2O exchg.); ^{13}C NMR (176 MHz, DMSO-d_6) δ (ppm): 14.0 (CH_3), 20.7 (CH_3), 56.4 (OCH_3), 60.6 (OCH_3), 104.7, 114.5, 116.5, 117.3, 120.6, 125.8, 126.3, 130.2, 133.0, 138.2, 139.6, 147.0, 148.3, 153.6, 165.9; MS: m/z = 433.49 [M]$^+$; $C_{25}H_{27}N_3O_4$.

2-(2,3-Dimethylanilino)-N'-[(E)-(4-hydroxy-3,5-dimethoxyphenyl) methylidene] benzohydrazide **(3)**

Yield: 80%; m. p.: 250–252 °C; FT-IR (KBr) ν cm^{-1}: 3292 (NH str.), 1662 (C=O), 1503 (C=N), 1320 (C-O); ^{1}H NMR (700 MHz, DMSO-d_6) δ (ppm): 2.13 (3H, s, CH_3), 2.29 (3H, s, CH_3), 3.83 (6H, s, 2×OCH_3), 6.81 (1H, t, J = 7 Hz, Ar-H), 6.86 (1H, d, J = 7 Hz, Ar-H), 6.95 (2H, d, J = 7 Hz, Ar-H), 6.99 (1H, s, Ar-H), 7.09 (2H, d, J = 7 Hz, Ar-H), 7.31 (1H, t, J = 7 Hz, Ar-H), 7.71 (1H, d, J = 7 Hz, Ar-H), 8.32 (1H, s, =CH), 8.93 (1H, s, OH), 9.22 (1H, s, NH, D_2O exchg.), 11.77 (1H, s, CONH, D_2O exchg.); ^{13}C NMR (176 MHz, DMSO-d_6) δ (ppm): 14.0 (CH_3), 20.7 (CH_3), 56.5 (OCH_3), 105.0, 114.5, 116.7, 117.3, 120.4, 125.0, 125.7, 126.3, 129.3, 130.0, 132.8, 138.2, 138.4, 139.5, 146.9, 149.0, 165.7; MS: m/z = 433.49 [M]$^+$; $C_{24}H_{25}N_3O$.

2-(2,3-Dimethylanilino)-N'-[(E)-(3,4-dimethoxyphenyl) methylidene] benzohydrazide **(4)**

Yield: 80%; m. p.: 255–257 °C; FT-IR (KBr) ν cm^{-1}: 3036 (NH str.), 1620 (C=O), 1503 (C=N), 1246 (C-O); ^{1}H NMR (700 MHz, DMSO-d_6) δ (ppm): 2.29 (3H, s, CH_3), 2.12 (3H, s, CH_3), 3.82 (6H, s, 2×OCH_3), 6.87 (2H, dd, J = 7 Hz, Ar-H), 6.96 (1H, s, Ar-H), 7.04 (1H, s, Ar-H), 7.09 (2H, s, Ar-H), 7.21 (1H, s, Ar-H), 7.30 (1H, d, J = 7 Hz, Ar-H), 7.36 (1H, s, Ar-H), 7.73 (1H, s, Ar-H), 8.37 (1H, s, =CH), 9.24 (1H, s, NH, D_2O exchg.), 11.79 (1H, s, CONH, D_2O exchg.); ^{13}C NMR (176 MHz, DMSO–d_6) δ (ppm): 14.0 (CH_3), 20.7 (CH_3), 55.9 (OCH_3), 56.0 (OCH_3), 108.6, 119.6, 114.5, 116.6, 117.3, 120.5, 122.4, 125.8, 126.3, 127.4, 129.3, 132.9, 138.2, 139.5, 146.9, 148.5, 149.5, 151.2, 165.7; MS: m/z = 403.47 [M]$^+$; $C_{24}H_{25}N_3O_3$.

2-(2,3-Dimethylanilino)-N'-[(E)-(2,3,4-trihydroxyphenyl) methylidene] benzohydrazide **(5)**

Yield: 80%; m. p.: 140–142 °C; FT-IR (KBr) ν cm^{-1}: 3243 (NH str.), 1627 (C=O), 1504 (C=N), 1220 (C-O); ^{1}H NMR (700 MHz, DMSO-d_6) δ (ppm): 2.28 (3H, s, CH_3), 2.31 (3H, s, CH_3), 6.79 (1H, J = 7 Hz, Ar-H), 6.84 (1H, d, J = 14 Hz, Ar-H), 7.06 (1H, d, J = 7 Hz, Ar-H), 7.11 (1H, s, Ar-H), 7.15 (1H, d, J = 7 Hz, Ar-H), 7.20 (1H, s, Ar-H), 7.33 (2H, t, J = 7 Hz, Ar-H), 7.57 (1H, s, =CH), 8.47 (1H, s, NH, D_2O exchg.), 9.18 (1H, s, CONH, D_2O exchg.); ^{13}C NMR (176 MHz, DMSO-d_6) δ (ppm): 207 (CH_3), 208 (CH_3), 88.4, 106.5, 113.4, 117.8, 121.6, 122.1, 126.5, 127.0, 127.3, 127.7, 128.9, 131.2, 133.2, 136.0, 138.5, 142.6, 145.0, 145.1, 155.3, 166.8, 167.4, 167.7, 168.2, 172.5; MS: m/z = 391.41 [M]$^+$; $C_{22}H_{21}N_3O_4$.

2-(2,3-dimethylanilino)-N'-[(E)-(2,4-dimethoxyphenyl) methylidene] benzohydrazide **(6)**

Yield: 80 %; m. p.: 213–215 °C; FT-IR (KBr) ν cm^{-1}: 3298 (NH str.), 1587 (C=O), 1499 (C=N), 1240 (C-O); ^{1}H NMR (700 MHz, DMSO-d_6) δ (ppm): 2.13 (3H, s, CH_3), 2.28 (3H, s, CH_3), 3.83 (3H, s, OCH_3), 3.87 (3H, s, OCH_3), 6.658 (2H, s, Ar-H), 6.79 (1H, t, J = 7 Hz, Ar-H), 6.86 (1H, d, J = 7 Hz, Ar-H), 6.94 (1H, d, J = 7Hz, Ar-H), 7.09 (2H, t, J = 7 Hz, Ar-H), 7.29 (1H, t, J = 7 Hz, Ar-H), 7.74 (1H, d, J = 7 Hz, Ar-H), 7.82 (1H, d, J = 7 Hz, Ar-H), 8.71 (1H, s, =CH), 9.33 (1H, s, NH, D_2O exchg.), 11.75 (1H, s, CONH, D_2O exchg.); ^{13}C NMR (176 MHz, DMSO-d_6) δ (ppm): 13.9 (CH_3), 20.7 (CH_3), 55.9 (OCH_3), 56.2 (OCH_3), 98.7, 106.8, 114.4, 115.6, 117.3, 120.3, 125.7, 126.3, 127.1, 129.3, 132.8, 138.1, 139.5, 143.9, 147.0, 159.6, 162.9, 165.6; MS: m/z = 403.47 $[M]^+$; $C_{24}H_{25}N_3O_3$.

General synthesis of final compounds **(7–12)**

A mixture of hydrazide derivatives **(1–6)** (0.002 mol) and excess of anhydrous acetic anhydride (10 mL) was refluxed for one hour. The acetic anhydride was distilled off and residue was poured into ice cold water. The solid was filtered and crystallized from ethanol to give final compounds **(7–12)**.

1-{5-[2-(2,3-Dimethylanilino) phenyl]-2-(2,4,5-trimethoxyphenyl)-1,3,4-oxadiazol-3(2H)-yl} ethan-1-one ***(7)***

Yield: 80%; Semisolid; FT-IR (KBr) ν cm^{-1}: 3298 (NH str.), 1587 (C=O), 1499 (C=N), 1240 (C-O); ^{1}H NMR (700 MHz, DMSO-d_6) δ (ppm): 2.20 (3H, s, CH_3), 2.25 (3H, s, CH_3), 2.31 (3H, s, $COCH_3$), 3.83 (3H, s, OCH_3), 3.78 (3H, s, OCH_3), 3.68 (3H, s, OCH_3), 6.77 (2H, t, J = 7Hz, Ar-H), 6.87 (1H, d, J = 7 Hz, Ar-H), 6.90 (1H, s, Ar-H), 7.05 (1H, d, J = 7 Hz, Ar-H), 7.15 (2H, d, J = 7 Hz, Ar-H), 7.20 (1H, d, J = 14 Hz, Ar-H), 7.30 (1H, t, J = 7Hz, Ar-H), 7.56 (1H, d, J = 7 Hz, Ha), 8.57 (1H, s, NH, D_2O exchg.); ^{13}C NMR (176 MHz, DMSO-d_6) δ (ppm): 14.1, 21.9, 31.4, 56.3, 57.0, 57.1, 88.3, 99.3, 107.4, 113.2, 115.5, 117.6, 122.0, 126.5, 128.9, 131.0, 132.7, 138.5, 143.0; MS: m/z = 475.53 $[M]^+$; $C_{27}H_{29}N_3O_5$.

1-{5-[2-(2,3-Dimethylanilino) phenyl]-2-(3,4,5-trimethoxyphenyl)-1,3,4-oxadiazol-3(2H)-yl} ethan-1-one ***(8)***

Yield: 80 %; Semisolid; 3290 (NH str.), 1578 (C=O), 1450 (C=N), 1230 (C-O); ^{1}H NMR (700 MHz, DMSO-d_6) δ (ppm): 2.08 (3H, s, CH_3), 2.14 (3H, s, CH_3), 2.30 (3H, s, $COCH_3$), 3.68 (3H, s, OCH_3), 3.78 (3H, s, OCH_3), 3.81 (3H, s, OCH_3), 6.75 (1H, s, Ar-H), 6.78 (1H, s, Ar-H), 6.86 (1H, d, J = 7 Hz, Ar-H), 7.04 (1H, d, J = 7 Hz, Ar-H), 7.07 (1H, s, Ar-H), 7.14 (1H, s, Ar-H), 7.19 (2H, d, J = 7 Hz, Ar-H), 7.29 (2H, d, J = 7 Hz, Ar-H), 7.56 (1H, s, Ar-H), 7.64 (1H, d, J = 7 Hz, Ar-H) 8.02 (1H, d, J = 7 Hz, Ha), 8.51 (1H, s, NH, D_2O exchg.); ^{13}C NMR (176 MHz, DMSO-d_6) δ (ppm): 14.1 (CH_3), 20.6 (CH_3), 31.0 ($COCH_3$), 56.3 (OCH_3), 60.4 (OCH_3), 63.6 (OCH_3), 90.8, 104.3, 105.0, 106.9, 113.3, 117.7, 122.1, 126.4, 128.9, 131.1, 132.4, 133.0, 138.6, 145.2, 153.5, 155.1, 167.3, 170.1, 172.5, 206.9; MS: m/z = 475.53 $[M]^+$; $C_{27}H_{29}N_3O_5$.

1-{5-[2-(2,3-Dimethylanilino) phenyl]-2-(4-hydroxy-3,5-dimethoxyphenyl)-1,3,4-oxadiazol-3(2H)-yl} ethan-1-one ***(9)***

Yield: 80%; Semisolid; 3278 (NH str.), 1590 (C=O), 1520 (C=N), 1220 (C-O); ^{1}H NMR (700 MHz, DMSO-d_6) δ (ppm): 2.19 (3H, s, CH_3), 2.26 (3H, s, CH_3), 2.31 (3H, s, $COCH_3$), 3.77 (6H, s, OCH_3), 6.79 (1H, t, J = 7 Hz, Ar-H), 6.87 (3H, t, J = 7 Hz, Ar-H), 7.05 (1H, d, J = 7 Hz, Ar-H), 7.11 (1H, s, Ar-H), 7.15 (1H, t, J = 7 Hz, Ar-H), 7.20 (1H, d, J = 7Hz, Ar-H), 7.32 (1H, m, Ar-H), 7.66 (1H, d, J = 7 Hz, Ha), 8.50 (1H, s, NH, D_2O exchg.); ^{13}C NMR (176 MHz, DMSO-d_6) δ (ppm): 14.1 (CH_3), 21.4 (CH_3), 31.1 ($COCH_3$), 56.6 (OCH_3), 63.6 (OCH_3), 68.7 (OCH_3), 90.6, 103.8, 113.3, 117.7, 122.1, 126.5, 129.0, 131.1, 133.1, 135.3, 138.5, 145.2, 152.5, 167.5, 168.4, 170.1, 170.8, 207.0; MS: m/z = 461.50 $[M]^+$; $C_{26}H_{27}N_3O_5$.

1-{5-[2-(2,3-Dimethylanilino) phenyl]-2-(3,4-dimethoxyphenyl)-1,3,4-oxadiazol-3(2H)-yl} ethan-1-one ***(10)***

Yield: 80%; Semisolid; 3280 (NH str.), 1578 (C=O), 1488 (C=N), 1210 (C-O); ^{1}H NMR (700 MHz, DMSO-d_6) δ (ppm): 2.19 (3H, s, CH_3), 2.28 (3H, s, CH_3), 2.32 (3H, s, $COCH_3$), 3.77 (6H, s, 2×OCH_3), 5.96 (1H, s, Ar-H), 6.79 (1H, t, J = 7 Hz, Ar-H), 6.86 (1H, d, J = 7 Hz, Ar-H), 7.01 (1H, d, J = 7Hz, Ar-H), 7.05 (1H, t, J = 7 Hz, Ar-H), 7.09 (1H, d, J = 7 Hz, Ar-H), 7.15 (1H, t, J = 7 Hz, Ar-H), 7.20 (1H, d, J = 7 Hz, Ar-H), 7.28 (1H, m, Ar-H), 7.62 (1H, d, J = 14 Hz, Ar-H), 8.10 (1H, d, J = 7 Hz, Ar-H), 8.52 (1H, d, J = 7 Hz, Ha), 8.96 (1H, s, NH, D_2O exchg.); ^{13}C NMR (176 MHz, DMSO-d_6) δ (ppm): 14.1 (CH_3), 20.7 (CH_3), 31.7 ($COCH_3$), 49.0 (OCH_3), 56.0 (OCH_3), 63.6, 68.7, 70.2, 90.7, 110.7, 112.2, 113.3, 117.7, 119.4, 123.0, 126.5, 126.8, 133.0, 136.6, 149.6, 151.0; MS: m/z = 445.51 $[M]^+$; $C_{26}H_{27}N_3O_4$.

1-{5-[2-(2,3-Dimethylanilino) phenyl]-2-(2,3,4-trihudroxyphenyl)-1,3,4-oxadiazol-3(2H)-yl} ethan-1-one ***(11)***

Yield: 80%; Semisolid; 3280 (NH str.), 1588 (C=O), 1488 (C=N), 1220 (C-O); ^{1}H NMR (700 MHz, DMSO-d_6) δ (ppm): 2.13 (3H, s, CH_3), 2.29 (3H, s, CH_3), 6.41 (1H, d, J = 7 Hz, Ar-H), 6.80 (2H, t, J = 7 Hz, Ar-H), 6.83 (1H, d, J = 7Hz, Ar-H), 6.96 (1H, d, J = 7 Hz, Ar-H), 7.10 (2H, t, J = 7 Hz, Ar-H), 7.31 (1H, t, J = 7 Hz, Ar-H), 7.75 (1H, d, J = 14 Hz, Ar-H), 8.48 (1H, s, Ha), 9.35 (1H, s, NH, D_2O exchg.), 9.52 (1H, s, OH, D_2O exchg.), 11.60 (1H, s, OH, D_2O exchg.), 12.01 (1H, s, OH, D_2O exchg.); ^{13}C NMR (176 MHz, DMSO-d_6) δ (ppm): 14.0 (CH_3), 20.7 (CH_3), 108.1, 111.3, 114.5, 115.5, 117.2, 120.8, 121.6, 126.0, 126.4, 129.2, 130.3, 133.1, 138.2, 139.3, 147.3, 148.0, 149.2, 150.6, 165.3; MS: m/z = 433.45$[M]^+$; $C_{24}H_{23}N_3O_5$.

1-{5-[2-(2,3-Dimethylanilino) phenyl]-2-(2,4-dimethoxyphenyl)-1,3,4-oxadiazol-3(2H)-yl} ethan-1-one ***(12)***

Yield: 80%; Semisolid; 3290 (NH str.), 1580 (C=O), 1490 (C=N), 1220 (C-O); ^{1}H NMR (700 MHz, DMSO-d_6) δ (ppm): 1.94 (3H, s, CH_3), 2.10 (3H, s, CH_3), 2.28 (3H, s, $COCH_3$), 3.88 (3H, s, OCH_3), 3.92 (3H, s, OCH_3), 6.64 (1H, d, J = 14 Hz, Ar-H), 6.69 (1H, s, Ar-H), 6.74 (1H, t, J = 7Hz, Ar-H), 6.81 (1H, d, J = 7 Hz, Ar-H), 6.95 (1H, t, J = 7 Hz, Ar-H), 7.08 (1H, d, J = 7 Hz,

Ar-H), 7.27 (1H, t, J = 14 Hz, Ar-H), 7.67 (2H, m, Ar-H), 9.27 (1H, s, Ha), 10.1 (1H, s, NH, D_2O exchg.); ^{13}C NMR (176 MHz, DMSO-d_6) δ (ppm): 13.9 (CH_3), 20.7 (CH_3), 21.2 ($COCH_3$), 56.2 (OCH_3), 56.4 (OCH_3), 98.6, 107.2, 114.2, 115.3, 117.1, 118.5, 120.7, 125.9, 126.3, 129.1, 130.2, 132.9, 138.2, 139.4, 164.9, 163.9, 166.5, 168.7, 169.1, 170.1, 187.7; MS: m/z = 445.51 $[M]^+$; $C_{26}H_{27}N_3O_4$.

Molecular docking

Ligand based drug likeness property and ADME/Toxicity prediction

The molecular structures of each ligand were analyzed and their compliance with Lipinski's rule of five was checked using the Swiss ADME server (http://www.swissadme.ch/). Various physicochemical properties of the ligands were also calculated using ORISIS property explorer. The ADME/T test was performed for each ligand, and their different pharmacokinetic and pharmacodynamic properties, including blood brain barrier permeability, human intestinal absorption, Cytochrome P (CYP) inhibitory potential, carcinogenicity, mutagenicity, Caco-2 permeability, etc., were predicted using the online server admet SAR (http://lmmd.ecust.edu.cn/admetsar2/) and server pkCSM (https://biosig.lab.uq.edu.au/pkcsm/).

Docking Method

Molecular modeling investigations were conducted using MOE 2015.10 software, which is provided by Chemical Computing Group Inc., located at 1010 Sherbrooke Street West, Suite 910, Montreal, QC. The crystal structures of the COX-1 and COX-2 enzymes were obtained from the protein data bank (PDB IDs 3N8Y and 5IKR, respectively, were complexed with diclofenac (DIF) and mefenamic acid (ID8)) the 3D structure of COX-1 and COX-2 were used with high resolution: 2.60 and 2.34 Å, respectively. Furthermore, the ligands in both crystals had structural fragments or moieties that resembled the test compounds. The protein structures were prepared for docking studies by correction of protein errors through the structure preparation procedure implemented in MOE. Initial steps involved assigning hydrogen positions according to default rules. Subsequently, all bound waters and cofactors present in the PDB file were eliminated. Lastly, employing the Gasteiger methodology, partial charges were computed, and the active site of the ensemble was defined as the amalgamation of residues within a 10.0 Å radius of the bound inhibitor. This active site encompassed the union of all ligands within the ensemble, considering all atoms situated less than 10.0 Å from any ligand atom.

The test molecules **(1–12)** were prepared by generating their 3D conformations using MOE-Builder from the molecular operating environment (MOE) version 2015.10. We defined the appropriate atom types (with hybridization states) and bond types, added hydrogen atoms, and assigned charges to each atom. Then, we minimized the structures' energy (MMFF94x, gradient: 0.01)[26]. Before that, we used the MOE program to minimize the ligand structures' energy with the AM1 method[27], a semi-empirical approach.

The prepared ligands were docked with the COX-1 and COX-2 enzymes using MOE version 2015.10. Each ligand was allowed to produce a maximum of 10 conformations using the default parameters of MOE (placement, triangle matcher; rescoring 1, London dG; refinement, force field; rescoring 2, GBVI/WSA ΔG). The top 300 conformations of the docked compounds were saved in a separate database. The most probable bioactive conformations of the ligands that interacted with the enzymes were identified based on their binding affinities and interactions. The ligand-receptor interactions of the docked compounds were evaluated using MOE scoring functions and visual inspection.

RESULTS AND DISCUSSION

Synthesis

The synthetic route used to synthesize the target compounds is described in (Scheme 1). Methyl-2-(2,3-dimethylphenylamino) benzoate **(ii)**, was prepared according to the method reported in the literature, using mefenamic acid as starting material[28]. The 2-(2,3-dimethylphenylamino) benzohydrazide **(iii)** was prepared by esterification of 2-(2,3-dimethylphenylamino) benzoic acid followed by treatment with hydrazine hydrate (99%) in absolute ethanol[29]. Reaction of the mefenamic hydrazide with different aldehydes in presence of ethanol and catalytic amount of glacial acetic acid resulted in hydrazones **(1–6)**[30–32]. The final compounds **(7–12)** were obtained by refluxing mefenamic hydrazones **(1–6)** with excess anhydrous acetic anhydride by a reported method[33]. All the compounds were obtained in good yield. The compounds were analyzed and characterized by spectral data. The purity of the compounds was checked by thin layer chromatography (TLC). In ^1H NMR spectroscopy of compounds **(1–6)**, NH proton was observed as broad singlet exchangeable proton at δ 8.47–9.33 *ppm* and CONH proton was observed as singlet exchangeable proton at δ 9.18–11.89 *ppm*. The =CH protons were observed as a singlet at δ 7.57-8.73 *ppm*. The methoxy protons and methyl protons were observed at δ 3.72–3.83 *ppm* and δ 2.13–2.29 *ppm* respectively. Similarly, in ^1H NMR spectroscopy of compounds **(7–12)**, the NH proton was observed as broad singlet exchangeable proton at δ 8.50–10.1 *ppm*. The =CH protons were observed as a singlet at δ 7.56–9.27 *ppm*. The methoxy protons and methyl protons were observed at δ 2.28–2.32 *ppm* and δ 1.94–2.2 *ppm* respectively. In ^{13}C NMR, all the compounds presented peaks for all carbon atoms at their respective positions. All the compounds were confirmed by molecular ion peaks according to their molecular weights in GC/MS analysis. The characterization of compounds by spectroscopic techniques confirmed the structure of prepared compounds **(1–12)**.

Docking study

The validation docking results of the co-crystal ligand (DIF) with (PDB ID 3N8Y) using MOE v. 2015 software revealed several important interaction details. The ligand showed H-bonding interactions with the OH group of TYR 385 (A) and the O atom of HOH 608 (A), with distances of 2.68 Å and 2.7 Å, respectively. In addition, it formed an H-bond with the OG atom of SER 530 (A) at a distance of 2.53 Å. The ligand also displayed π-π

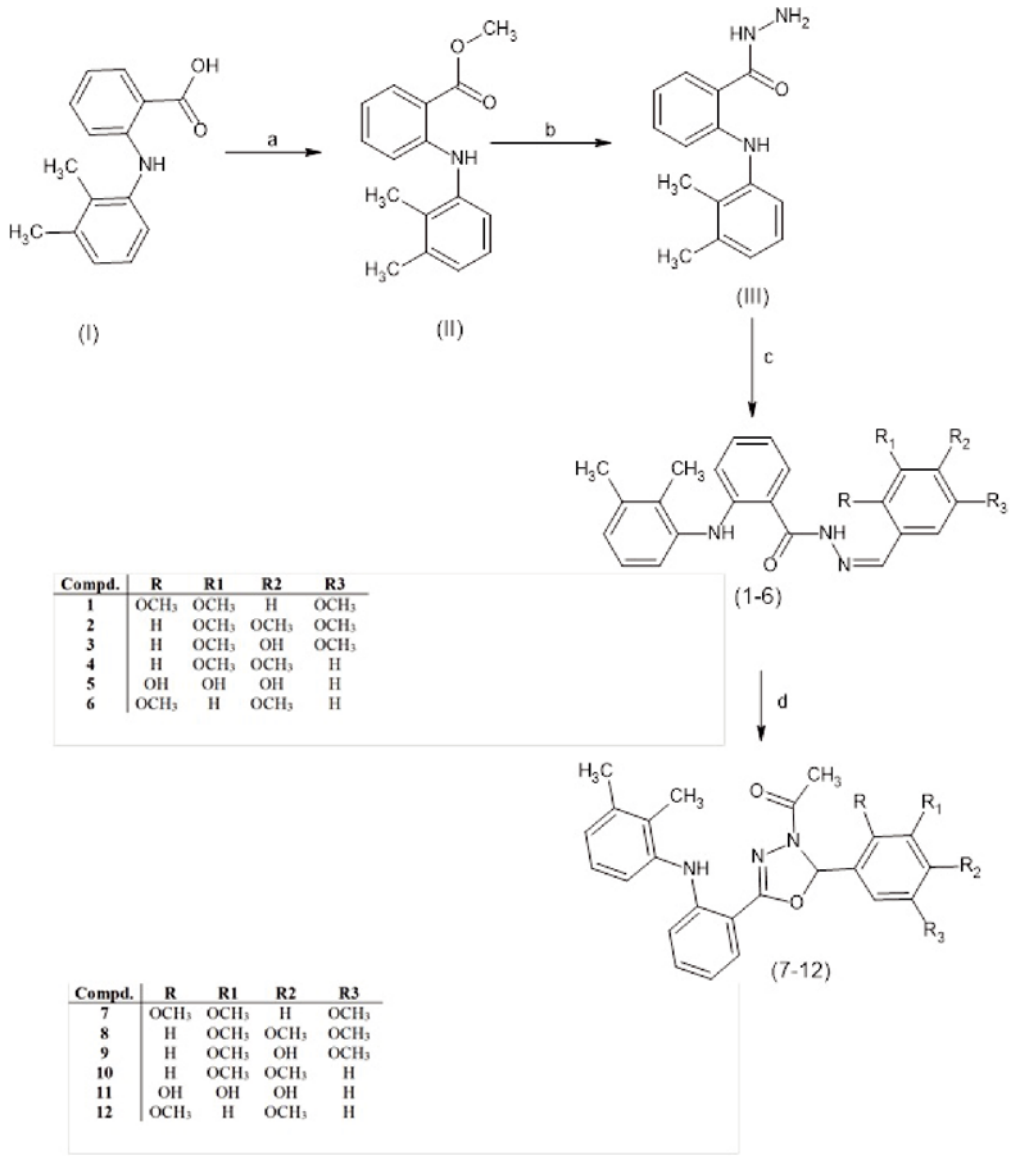

Compd.	R	R1	R2	R3
1	OCH_3	OCH_3	H	OCH_3
2	H	OCH_3	OCH_3	OCH_3
3	H	OCH_3	OH	OCH_3
4	H	OCH_3	OCH_3	H
5	OH	OH	OH	H
6	OCH_3	H	OCH_3	H

Compd.	R	R1	R2	R3
7	OCH_3	OCH_3	H	OCH_3
8	H	OCH_3	OCH_3	OCH_3
9	H	OCH_3	OH	OCH_3
10	H	OCH_3	OCH_3	H
11	OH	OH	OH	H
12	OCH_3	H	OCH_3	H

Scheme 1. Reaction for the synthesis of novel 1,3,4-oxadiazole derivatives of mefenamic acid. Conditions for the reaction, (a) MeOH, sulfuric acid, reflux 18 hours (b) EtOH, hydrazine hydrate, reflux 12 hours (c) RCHO, glacial acetic anhydride, EtOH, reflux 3 hours (d) Anhydrous acetic anhydride, reflux one hour

stacking interactions with the 6-ring of TYR 385 (A) and CD1 of LEU 352 (A), with distances of 4.76 Å and 4.23 Å, respectively (Fig. 1). The RMSD value of 0.345 indicates that the docking results are reliable. Overall, the successful validation of the docking protocol using the PDB ID 3N8Y and MOE v. 2015 software provides a solid foundation for further studies and can be utilized to predict the binding of new ligands with the target protein.

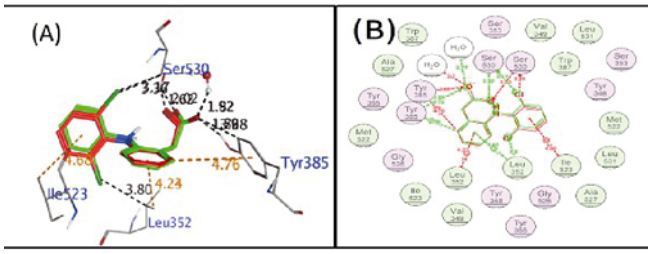

Figure 1. Comparison between the co-crystallized pose (in red) and the re-docked pose (in green) of the diclofenac (DIF) within human cyclooxygenase-1 (PDB ID: 3N8Y)

Docking study of compounds (1–6) with COX-1

Compound **1** forms multiple hydrophobic interactions with the enzyme, including H-pi interactions with TYR 385 and TYR 355, as well as pi-H interactions with VAL 349 and PHE 381. The ligand-receptor interaction distance is 4.09 Å, and the scoring energy is -0.2 kcal/mol. Compound **2** also forms H-pi interactions with TYR 385 and pi-H interactions with LEU 352 and GLY 526. The ligand-receptor interaction distance is 4.72 Å, and the scoring energy is –0.3 kcal/mol. Compound **3** has similar interactions as compound **2**, but forms a stronger H-pi interaction with PHE 209. The ligand-receptor interaction distance is 4.66 Å, and the scoring energy is –0.5 kcal/mol. Compound **4** forms an H-acceptor interaction with SER 530 and pi-H interactions with LEU 352 and GLY 526. The ligand-receptor interaction distance is 2.98 Å, and the scoring energy is –0.7 kcal/mol. Compound **5** forms H-pi interactions with TYR 385, pi-H interactions with GLY 526, and a pi-H interaction with a water molecule (HOH 588). The ligand-receptor interaction distance is 4.84 Å, and the scoring energy is –0.4 kcal/mol. Compound **6** has a strong H-acceptor interaction with SER 530, as well as pi-H interactions with LEU 352

and GLY 526. The ligand-receptor interaction distance is 2.95 Å, and the scoring energy is –1.2 kcal/mol. Reference compound (DIF) forms H-acceptor interactions with TYR 385, water molecule (HOH 608), and SER 530, as well as pi-H interactions with TYR 385 and LEU 352. The ligand-receptor interaction distance is 2.68 Å, and the scoring energy is –4.9 kcal/mol. Docking results of compounds (**1–6**) and reference compound diclofenac with the COX-1 enzyme are presented in (Table 1). Overall, the test compounds showed varying degrees of binding affinity with the COX-1 enzyme, with compound **4** and DIF having the strongest interactions.

The docking of compounds (7–12) with the COX-1 enzyme

The docking simulations revealed that all compounds exhibited strong binding affinity towards COX-1, as evidenced by their high negative scoring values (Table 2). Among the compounds, compound **10** demonstrated the highest binding affinity with a scoring value of –9.851 kcal/mol. This compound formed H-acceptor interactions with CG2 of VAL349 and H-pi interactions with TYR385 and PHE205. Additionally, it formed pi-H interactions with CG1 of VAL349, CD1 of LEU352, and ILE523, as well as a pi-H interaction with CA of GLY526. These interactions contribute to the stability and favorable binding of compound **10** within the COX-1 binding site (Fig. 2). Compound **7** displayed the second highest binding affinity with a scoring value of –9.486 kcal/mol. It formed H-acceptor interactions with CH2 of TRP387 and H-pi interactions with CE2 of PHE205 and CD1 of LEU352. Furthermore, it formed a pi-H interaction with OH of TYR385, further contributing to its binding stability. Compound **12** exhibited the third highest binding affinity with a scoring value of –9.406 kcal/mol. It formed H-donor interactions with OG of SER530 and a pi-H interaction with CD1 of LEU352. Moreover, it formed

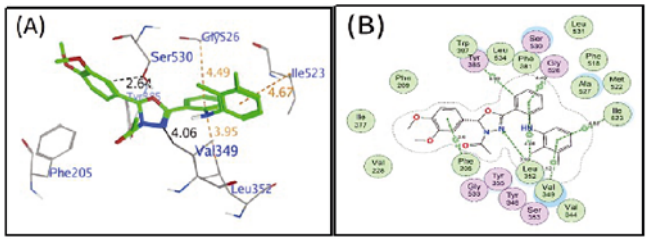

Figure 2. Interactions of compound 10 with amino acid residues situated within the catalytic domain of human cyclooxygenase-1 (PDB ID: 3N8Y).

pi-H interactions with CA of GLY526 and SER530, reinforcing its binding to COX-1. These top three potent compounds, **10**, **7**, and **12**, showed promising binding interactions with COX-1, suggesting their potential as COX-1 inhibitors. Compounds, **8**, **9**, and **11**, also showed promising interactions with COX-1, suggesting their potential as COX-1 inhibitors. While their binding affinities were slightly lower than the top three compounds, they still exhibited favorable interactions with important residues within the active site. However, it is important to note that these findings are based on computational docking simulations, and further experimental studies are necessary to validate their binding affinities and evaluate their functional activities.

Overall, the docking results suggest that all six compounds have the potential to bind to the COX-1 enzyme, with compound **10** having the highest potential for binding.

Docking of compounds (1–6) with COX-2

Here, we have docked six compounds (**1–6**) with the COX-2 enzyme (5IKR.pdb). The docking results are presented in the (Table 3) with details of the interactions, distances, and energies. All six compounds have interacted with the ARG 120 residue of COX-2 through H-bonding

Table 1. Molecular docking interactions between COX-1 enzyme (PDB ID: 3N8Y) and investigated compounds (1–6) as well as reference diclofenac (DIF).

Compd.	Ligand	Receptor	Interaction	Distance	E (kcal/mol)	Scoring (kcal/mol)
1	C 1	6-ring TYR 385 (A)	H-pi	4.09	–0.2	–6.433
	C 20	6-ring TYR 355 (A)	H-pi	4.69	–0.3	
	C3 54	6-ring PHE 209 (A)	H-pi	4.12	–0.5	
	6-ring	CG1 VAL 349 (A)	pi-H	3.47	–0.2	
	6-ring	CE1 PHE 381 (A)	pi-H	4.75	–0.2	
2	C 1	6-ring TYR 385 (A)	H-pi	4.72	–0.3	–7.099
	C 39	6-ring PHE 209 (A)	H-pi	4.64	–0.5	
	6-ring	CD1 LEU 352 (A)	pi-H	3.94	–0.3	
	6-ring	CA GLY 526 (A)	pi-H	4.74	–0.3	
3	C 1	6-ring TYR 385 (A)	H-pi	4.66	–0.5	–7.411
	C 53	6-ring PHE 209 (A)	H-pi	3.43	–0.5	
	6-ring	CD1 LEU 352 (A)	pi-H	3.95	–0.3	
	6-ring	CA GLY 526 (A)	pi-H	4.76	–0.3	
4	O1 19	OG SER 530 (A)	H-acceptor	2.98	–0.7	–8.477
	6-ring	CD1 LEU 352 (A)	pi-H	4.31	–0.7	
	6-ring	CA GLY 526 (A)	pi-H	4.47	–0.2	
5	C 1	6-ring TYR 385 (A)	H-pi	4.84	–0.4	–8.521
	6-ring	CA GLY 526 (A)	pi-H	4.86	–0.3	
	6-ring	O HOH 588 (A)	pi-H	4.75	–0.3	
6	O1 19	OG SER 530 (A)	H-acceptor	2.95	–1.2	–8.249
	6-ring	CD1 LEU 352 (A)	pi-H	4.05	–0.6	
	6-ring	CA GLY 526 (A)	pi-H	4.55	–0.5	
DIF	O1 28	OH TYR 385 (A)	H-acceptor	2.68	–4.9	–8.198
	O1 28	O HOH 608 (A)	H-acceptor	2.7	–3.5	
	O2 29	OG SER 530 (A)	H-acceptor	2.53	–2.2	
	C12 22	6-ring TYR 385 (A)	H-pi	4.76	–0.3	
	6-ring	CD1 LEU 352 (A)	pi-H	4.23	–0.4	

Table 2. Molecular docking interactions between COX-1 Enzyme (PDB ID: 3N8Y) and compounds (7–12)

Compd.	Ligand	Receptor	Interaction	Distance	E (kcal/mol)	Scoring (kcal/mol)
7	N 34	CH2 TRP 387 (A)	H-acceptor	3.96	–0.2	–9.486
	6-ring	CE2 PHE 205 (A)	pi-H	3.79	–0.2	
	6-ring	CD1 LEU 352 (A)	pi-H	4.09	–0.5	
	6-ring	OH TYR 385 (A)	pi-H	4.46	–0.3	
8	N 34	CH2 TRP 387 (A)	H-acceptor	3.94	–0.2	–9.026
	6-ring	CE2 PHE 205 (A)	pi-H	3.59	–0.2	
	6-ring	CD1 LEU 352 (A)	pi-H	4.25	–0.6	
	6-ring	CZ PHE 381 (A)	pi-H	3.56	–0.3	
	6-ring	CA GLY 526 (A)	pi-H	4.28	–0.4	
9	N 34	CE2 TYR 348 (A)	H-acceptor	3.25	–0.2	–9.310
	N 34	OH TYR 385 (A)	H-acceptor	2.65	–0.4	
	6-ring	CD1 LEU 352 (A)	pi-H	4.72	–0.6	
10	N 34	CG2 VAL 349 (A)	H-acceptor	3.99	–0.2	–9.851
	C 1	6-ring TYR 385 (A)	H-pi	4.69	–0.2	
	6-ring	CE2 PHE 205 (A)	pi-H	3.6	–0.2	
	6-ring	CG1 VAL 349 (A)	pi-H	3.52	–0.2	
	6-ring	CD1 LEU 352 (A)	pi-H	4.08	–0.5	
	6-ring	CG2 ILE 523 (A)	pi-H	4.83	–0.3	
	6-ring	CA GLY 526 (A)	pi-H	4.49	–0.3	
11	C 30	OG SER 530 (A)	H-donor	3.19	–0.3	–8.521
	O 51	O SER 530 (A)	H-donor	2.85	–1.5	
	6-ring	CD1 LEU 352 (A)	pi-H	4.32	–0.6	
	6-ring	CA GLY 526 (A)	pi-H	4.3	–0.3	
	6-ring	O HOH 588 (A)	pi-H	4.79	–0.2	
12	C 30	OG SER 530 (A)	H-donor	3.14	–0.2	–9.406
	6-ring	CD1 LEU 352 (A)	pi-H	4.33	–0.4	
	6-ring	CA GLY 526 (A)	pi-H	4.3	–0.4	
	6-ring	CA SER 530 (A)	pi-H	3.72	–0.2	

Table 3. Molecular docking interactions between COX-2 Enzyme (PDB ID: 5IKR) and compounds (1–6)

Compd.	Ligand	Receptor	Interaction	Distance	E (kcal/mol)	Scoring (kcal/mol)
1	N1 15	NH2 ARG 120 (A)	H-acceptor	2.95	–4.9	–6.832
	6-ring	CG2 VAL 116 (A)	pi-H	3.3	–0.3	
	6-ring	CG1 VAL 349 (A)	pi-H	3.31	–0.2	
	6-ring	CA GLY 526 (A)	pi-H	4.11	–0.3	
2	C 23	SD MET 522 (A)	H-donor	4.39	–0.2	–8.487
	N1 15	NH2 ARG 120 (A)	H-acceptor	3.2	–3.4	
3	N1 15	NH2 ARG 120 (A)	H-acceptor	2.97	–4.8	–8.523
	6-ring	CG2 VAL 116 (A)	pi-H	4.92	–0.2	
	6-ring	CA VAL 523 (A)	pi-H	4.9	–0.4	
	6-ring	CA ALA 527 (A)	pi-H	4.42	–0.2	
4	N1 15	NH2 ARG 120 (A)	H-acceptor	3	–4.1	–6.883
	6-ring	CB ALA 527 (A)	pi-H	4.74	–0.4	
5	N1 15	NH2 ARG 120 (A)	H-acceptor	3.24	–3.6	–7.769
	6-ring	CA VAL 523 (A)	pi-H	4.84	–0.4	
	6-ring	CA ALA 527 (A)	pi-H	4.36	–0.2	
6	N1 15	NH2 ARG 120 (A)	H-acceptor	2.97	–5.5	–8.194
	C 23	6-ring PHE 518 (A)	H-pi	4.5	–0.4	
	6-ring	CD1 LEU 93 (A)	pi-H	3.89	–0.2	
	6-ring	CG2 VAL 116 (A)	pi-H	3.99	–0.2	
	6-ring	CG LEU 531 (A)	pi-H	3.81	–0.2	

with the NH_2 group of the ligand. Additionally, compounds **1**, **3, 4, 5,** and **6** have shown interactions with other important residues such as VAL 116, VAL 349, GLY 526, MET 522, VAL 523, ALA 527, PHE 518, LEU 93, and LEU 531 through pi-H or H-pi interactions. Comparing the docking results, compound **3** and **6** have shown the highest negative S values (–8.523 kcal/mol and –8.194 kcal/mol, respectively) (Fig. 3), indicating their higher binding affinity towards COX-2. Compounds **1, 4,** and **5** have also shown significant binding energies ranging from –6.832 kcal/mol to –7.769 kcal/mol. Compound **1** has shown the lowest binding energy of -6.832 kcal/mol, which is still within the acceptable range. In summary, the docking results suggest that all six compounds have the potential to bind with COX-2 enzyme through various interactions with important residues. Compounds **3** and **6** have shown the highest binding affinities among the six compounds, followed by **2, 4,** and **5**. Further experimental studies are required to validate the predictions of the docking results.

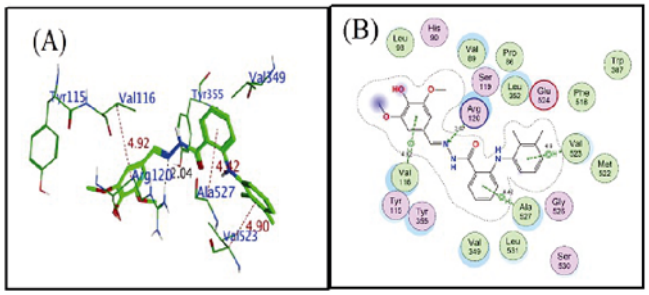

Figure 3. Compound 3 interactions with amino acid residues in the catalytic domain of human cyclooxygenase-2 (PDB ID: 5IKR)

Docking of compounds (7–12) with COX-2

Compound **7** has several interactions with the COX-2 enzyme, including H-acceptor interaction with TRP 387, pi-H interactions with PHE 205, LEU 352, and TYR 385. The distance between the ligand and the receptor is 3.96, and the energy score is –0.2 kcal/mol. These interactions suggest that Compound **7** may have the potential to bind to the Cox-2 enzyme. Compound **8** has multiple interactions with the Cox-2 enzyme, including H-acceptor interaction with TRP 387, pi-H interactions with PHE 205, LEU 352, PHE 381, and GLY 526. The distance between the ligand and the receptor is 3.94, and the energy score is –0.2 kcal/mol. These results suggest that Compound **8** may also have the potential to bind to the Cox-2 enzyme. Compound **9** has H-acceptor interactions with TYR 348 and TYR 385, as well as a pi-H interaction with LEU 352. The distance between the ligand and the receptor is 3.25, and the energy score is –0.2 kcal/mol. These interactions suggest that compound **9** may have moderate potential to bind to the Cox-2 enzyme. Compound **10** has several interactions with the Cox-2 enzyme, including H-acceptor interaction with VAL 349 and H-pi interaction with TYR 385. Additionally, it has pi-H interactions with PHE 205, VAL 349, LEU 352, ILE 523, and GLY 526. The distance between the ligand and the receptor is 3.99, and the energy score is –0.2 kcal/mol. These interactions suggest that Compound **10** may have high potential to bind to the Cox-2 enzyme. Compound **11** has H-donor interactions with SER 530, as well as pi-H interactions with LEU 352, GLY 526, and HOH 588. The distance between the ligand and the receptor is 3.19, and the energy score is –0.3 kcal/mol. These interactions suggest that Compound **11** may have moderate potential to bind to the Cox-2 enzyme. Compound **12** has H-acceptor interactions with VAL 349 and TYR 385, as well as pi-H interactions with PHE 205, LEU 352, ILE 523, and GLY 526. The distance between the ligand and the receptor is 3.87, and the energy score is –0.3 kcal/mol. These interactions suggest that compound **12** may have moderate to high potential to bind to the Cox-2 enzyme. Overall, the docking results suggest that all six compounds have the potential to bind to the Cox-2 enzyme, with compound **10** having the highest potential for binding (Fig. 4).

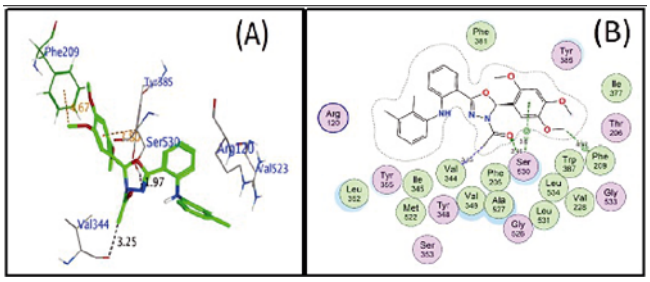

Figure 4. : Interactions of compound 10 with amino acid residues within the catalytic domain of human cyclooxygenase-2 (PDB ID: 5IKR)

In this case, we have six compounds **(7–12)** docked with COX-2 enzyme (5IKR.pdb), and the results are summarized in the (Table 4). Compound **10** showed the highest scoring value (–8.724 kcal/mol), indicating a strong interaction with the COX-2 enzyme. It formed hydrogen bonds with TYR385 and had pi interactions with PHE205, SER530, and TYR355. These residues are known to be important for the function of the COX-2 enzyme, and their interaction with compound **10** suggests that it could be a potential inhibitor of COX-2 activity. Compound **7, 8, 9,** and **12** also showed significant interaction with the COX-2 enzyme, with scoring values ranging from –5.416 kcal/mol to –4.679 kcal/mol. These compounds formed hydrogen bonds with VAL344, SER353, MET522, and SER530, respectively, and also had pi interactions with important residues such as ARG120, TYR385, PHE209, and TYR348. Compound **11** had a moderate interaction

Table 4. Molecular docking interactions between COX-2 Enzyme (PDB ID: 5IKR) and compounds (7–12)

Compd.	Ligand	Receptor	Interaction	Distance	E (kcal/mol)	Scoring (kcal/mol)
7	C21 37	O VAL 344 (A)	H-donor	3.25	–0.2	–5.416
	O23 41	OG SER 530 (A)	H-acceptor	2.46	–0.3	
	C 50	6-ring PHE 209 (A)	H-pi	4.67	–0.2	
	6-ring	CA SER 530 (A)	pi-H	3.8	–0.3	
8	C21 37	O SER 353 (A)	H-donor	3.54	–0.2	–4.517
	6-ring	NE ARG 120 (A)	pi-cation	4.09	–0.2	
	6-ring	OG SER 530 (A)	pi-H	4.91	–0.2	
9	C 3	SD MET 522 (A)	H-donor	4.18	–0.3	–4.954
	C 47	O SER 530 (A)	H-donor	3.52	–0.2	
	O23 41	OH TYR 385 (A)	H-acceptor	2.92	–0.3	
	C 26	6-ring TYR 355 (A)	H-pi	4.28	–0.2	
10	N 34	OH TYR 385 (A)	H-acceptor	2.59	–1.3	–8.724
	C 13	6-ring TYR 355 (A)	H-pi	4.67	–0.3	
	6-ring	CE2 PHE 205 (A)	pi-H	3.53	–0.6	
	6-ring	CA SER 530 (A)	pi-H	3.66	–0.6	
11	N 34	OH TYR 385 (A)	H-acceptor	2.93	–0.2	–5.625
12	C 3	SD MET 522 (A)	H-donor	4.4	–0.3	–4.679
	C21 37	O SER 530 (A)	H-donor	3.48	–0.2	
	C 44	6-ring PHE 205 (A)	H-pi	3.34	–0.2	
	6-ring	CG1 VAL 523 (A)	pi-H	4.94	–0.3	
	6-ring	6-ring TYR 348 (A)	pi-pi	3.75	0	
ID8	O16 1	OH TYR 385 (A)	H-acceptor	2.82	–2.7	–7.282
	O16 1	O HOH 750 (A)	H-acceptor	3.02	–1.8	
	O15 3	OG SER 530 (A)	H-acceptor	2.77	–1.2	
	C12 5	6-ring TYR 385 (A)	H-pi	4.61	–0.2	
	C3 16	6-ring TYR 355 (A)	H-pi	4.74	–0.3	
	6-ring	CA GLY 526 (A)	pi-H	4.02	–0.3	

with the COX-2 enzyme, with a scoring value of –5.625 kcal/mol. It formed a hydrogen bond with TYR385, which is one of the key residues involved in the catalytic activity of COX-2. Overall, the docking results suggest that these compounds could potentially inhibit the activity of the COX-2 enzyme by binding to the active site and interfering with the substrate binding. Further studies, such as *in vitro* and *in vivo* experiments, are needed to validate these findings and determine the actual potency of these compounds as COX-2 inhibitors.

The docking of the co-crystalline ligand ID8 with the COX-2 enzyme (5IKR.pdb) resulted in specific interactions between the ligand and important residues of the receptor. ID8 formed hydrogen bonds with TYR385 and SER530, which are known to be critical for the catalytic activity of COX-2. It also had pi interactions with TYR385, TYR355, and GLY526. These interactions indicate that ID8 can bind effectively to the active site of COX-2 and potentially inhibit its activity. The successful validation of the docking protocol using the co-crystalline ligand ID8 strengthens the reliability of the docking methodology employed. It demonstrates that the docking protocol is capable of accurately predicting the binding mode and interactions of ligands with the COX-2 enzyme. To evaluate the protocol further and compare the results with compounds **(1–12)**, we can consider the similarity and differences in their interactions and scoring values. Comparing the interactions observed for ID8 with those of **(1–12)**, we can identify common interaction patterns that are crucial for the binding of ligands to COX-2. For example, hydrogen bonding with TYR385 and SER530 appears to be a common feature across multiple ligands (Figure 5 A & B). This suggests that these interactions play a significant role in the binding of ligands to the active site of COX-2. Additionally, the scoring values can be used as a measure of the binding affinity of the ligands. By comparing the scoring values of ID8 with those of **(1–12)**, we can assess the relative potency of the compounds. Ligands with lower scoring values generally indicate stronger binding affinity. Based on the provided data, compound **10** exhibited the highest scoring value (–8.724 kcal/mol) among the compounds, followed by ID8 (–7.282 kcal/mol). This suggests that Compound **10** and ID8 have a relatively stronger binding affinity to COX-2 compared to the other compounds.

Individual molecular docking of the test compounds into the active sites of both cyclooxygenase-1 (COX-1) and cyclooxygenase-2 (COX-2) was executed, demonstrating successful interactions evidenced by the formation of complexes between COX-1 and COX-2 with the ligands. The visualization of hydrogen-bond interactions, binding energy, bond length, active site residues, and the orientation of the docked compounds within the active sites was conducted.

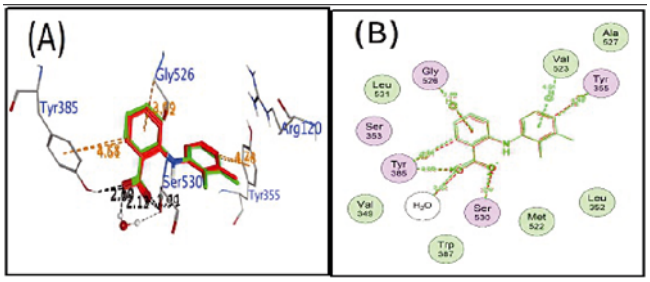

Figure 5. Comparison between the co-crystallized pose (red) and the re-docked pose (green) of mefenamic acid within human cyclooxygenase-2 (PDB ID: 5IKR)

Among the screened test compounds **(7–12),** those exhibiting the most favorable orientation were identified based on interactions with key residues in the active site, including SER 530, ARG 120, TYR 385, and VAL 523. Analysis of ΔG values revealed predominantly negative and low values, indicating robust and favorable bonding between COX and the ligands in their optimal conformations. The binding energies for test compounds 7–12, along with the standard drug diclofenac, with COX-1 were determined as –9.486, –9.026, –9.31, –9.851, –8.521, –9.406, and –8.198 kcal mol-1, while with COX-2, the values were –5.416, –4.517, –4.954, –8.724, –5.625, –4.679, and –7.282 kcal mol−1, respectively. These results suggest a higher affinity of the test compounds for COX-1. Furthermore, in-depth analysis reveals that compound 10 stands out prominently, being predicted as highly potent in binding with COX-1, as evidenced by its exceptionally low binding energy of –9.851 kcal mol-1, underscoring its potential therapeutic relevance.

In conclusion, the *in-silico* studies unambiguously predict a robust interaction between the selected test compounds and COX-1, emphasizing their preferential association with COX-1 over COX-2.

Predicting Drug-Likeness and ADMET Properties

Drug-likeness

The drug-likeness of the compounds was analyzed based on several physicochemical properties, including molecular weight, rotatable bonds, H-bond donors/acceptors, aromatic atoms, consensus LogP, and solubility (Table 5). Compound **5** was found to be the most drug-like compound due to its relatively low molecular weight, fewer rotatable bonds, more H-bond donors,

Table 5. Drug-likeness properties of compounds (1–12)

Compd.	Molecular weight	Log P	H-bond donors	H-bond acceptors	Rotatable bonds	PSA
1	433.5	3.49	2	5	9	81.18
2	433.5	3.78	2	5	9	81.18
3	419.47	3.38	3	5	8	92.18
4	403.47	3.25	2	4	8	71.95
5	391.42	1.58	5	5	6	114.18
6	403.47	3.62	2	4	8	71.95
7	475.54	4.4	1	6	8	81.62
8	475.54	4.64	1	6	8	81.62
9	461.51	4.07	2	6	7	92.62
10	445.51	4.12	1	5	7	72.39
11	433.46	3.47	4	6	5	114.62
12	445.51	4.04	1	5	7	72.39

and highest predicted solubility. Compound **3** was also considered drug-like, while the other compounds may face challenges with poor solubility and high lipophilicity. Lipinski's rule of five and Veber's Rule were also applied to predict the drug-likeness of the compounds. Lipinski's rule of five was satisfied by all the compounds, as they had molecular weights low than 500 g/mol, but the majority had Log P values ≤ 5, and fewer H-bond donors and acceptors. Veber's rule was satisfied by all the compounds, as they had less than 10 rotatable bonds and less than 10 polar groups. In conclusion, based on both Lipinski's rule of five and Veber's rule, all the compounds can be considered drug-like. However, further optimization and testing would be required to determine the most promising drug candidate.

ADMET: The ADMET (absorption, distribution, metabolism, excretion, and toxicity) data for the given compounds are shown in the (supplementary file).

A (Absorption): The predicted scores for all compounds range from 0.7222 to 0.9588, indicating a high potential for efficient human intestinal absorption and entry into the systemic circulation. The commonly used *in vitro* method, Caco-2 permeability, predicts the intestinal absorption of drugs, and the compounds have varied predictions for this method. However, all compounds with high scores (above 0.5) are expected to be well--absorbed. The oral bioavailability of a drug depends on its ability to reach the systemic circulation after oral administration. In this case, all compounds have good oral bioavailability, with scores above 0.5.

D (Distribution): Regarding the steady state volume of distribution (VDss), which represents the volume of distribution at steady state, compounds with a log VDss less than –0.15 are considered to have low VDss values, while those with log VDss greater than 0.45 are considered to have high VDss values. Based on this criterion, it can be seen that all 12 compounds have low VDss values since their log VDss values range from –0.661 to –0.053. This suggests that these compounds are mostly confined to the bloodstream and have limited distribution into tissues. All of the compounds are predicted to cross the BBB to some degree, with varying scores ranging from –0.575 to +0.8. This suggests that the compounds may have some ability to penetrate the central nervous system and potentially affect brain function. In terms of P-glycoprotein (P-gp) interaction, all of the compounds are predicted to be P-gp inhibitors to varying degrees, with scores ranging from 0.721 to 0.9653. This means that the compounds may inhibit the function of P-gp, a transporter protein that pumps drugs out of cells, potentially increasing their bioavailability and enhancing their therapeutic effect. In terms of P-gp substrate potential, all of the compounds are predicted to be P-gp substrates to some extent, with scores ranging from –0.5855 to 0.5157. This suggests that the compounds may be recognized by P-gp and transported out of cells, potentially reducing their effectiveness.

M (Metabolism): Compounds **(1–6)** and compounds **(7–12)** in terms of their inhibition of transporters (OATP1B1, OATP1B3, and BSEP) and metabolism by different enzymes (CYP3A4 and CYP2C9). Compounds **(1–12)** show inhibition of transporters and metabolism by CYP3A4, indicating potential for drug-drug interactions. Compound **3** and compound **9** show metabolism by CYP2C9 as well. Compound **4** and compound **10** do not show strong inhibition of any transporters or metabolism by any CYPs, while compound **5** and compound **11** do not show strong inhibition of any transporters but do show some metabolism by CYP3A4.

E (Excretion): Based on the given results, the total clearance values for the twelve compounds range from –0.051 to 0.407 log ml/min/kg. The clearance value represents the rate at which a compound is removed from the body and is influenced by factors such as metabolism and excretion. A positive clearance value suggests that a compound is eliminated from the body at a faster rate, while a negative value suggests that the compound is retained in the body for a longer time. Considering the range of clearance values obtained, it can be inferred that some of the compounds are cleared more efficiently than others. For instance, compound **5** has a negative clearance value of –0.051, indicating that it is retained in the body for a longer time. On the other hand, compound **1** has the highest clearance value of 0.407, suggesting that it is cleared from the body relatively quickly.

T (Toxicity): Based on the results, it can be concluded that none of the analogs were predicted to be carcinogenic using the binary model, and all analogs were predicted to be non-required for the endpoint in the trinary model. None of the analogs were predicted to be corrosive to the eyes, while compound **1**, **3**, **5**, and **11** were predicted to be mutagenic, and the remaining analogs were predicted to be non-mutagenic. Most of the analogs were predicted to inhibit the hERG channel, with compound **3** and **9** having the highest inhibition scores. Furthermore, all analogs except compound **11** were predicted to have no adverse effects on the reproductive system. These results can be useful in guiding further research and development of these analogs and in assessing their safety for various applications.

CONCLUSION

In conclusion, a novel series of compounds containing 1,3,4-oxadiazole derivatives of mefenamic acid was obtained in good to moderate yield. The mefenamic hydrazide was obtained by reacting methyl ester of mefenamic acid with hydrazine hydrate. The mefenamic acid hydrazones were obtained by reacting different substituted aldehydes with mefenamic acid hydrazide. Finally, the 1,3,4-oxadiazole derivatives of mefenamic were obtained by reacting substituted hydrazones with excess anhydrous acetic anhydride. The synthesized compounds were purified by recrystallization from ethanol. All the compounds were analyzed characterized fully by spectral data like FT-IR, ^{1}H NMR, ^{13}C NMR and mass spectroscopy which confirmed the molecular structure of synthesized compounds. Molecular docking studies of all the compounds were performed against COX-1/COX-2 enzymes. The successful docking validation of ID8 with COX-2 demonstrates the reliability of the docking protocol used and RMSD was 0.227 Å. The comparison of the interactions and scoring values with other compounds provides insights into the common features and relative potency of the ligands. Compound **4** and compound **10** were found to be highest potential

to bind with COX-1 while as compound **3**, compound **6** and compound **10** were found to have highest potential to bind with COX-2 enzyme. These findings can guide the selection of potential COX-2 inhibitors for further evaluation and development.

ACKNOWLEDGMENTS

The authors extend their appreciation to the Deputyship for Research and Innovation, Ministry of Education in Saudi Arabia for funding this research work through the project no. (IFKSUOR3–352-2).

LITERATURE CITED

1. Syed, M.M., Parekh, A.B. & Tomita, T. (1990). Receptors involved in mechanical responses to catecholamines in the circular muscle of guinea-pig stomach treated with meclofenamate. *Brit. J. Pharm.* 101, 809–814. DOI: 10.1111/j.1476-5381.1990.tb14162.x.

2. Belsole, S.C. (1986). Meclofenamic acid topical pharmaceutical composition. *US Patent* 4602040.

3. Martindale, J.E.F. (1996). The extra pharmacopoeia, 31st ed.; Reynolds Ed.; The Pharmaceutical Press: London, UK.

4. Metz, G. (1990). Method of producing 2-(2-hydroxyethoxy)-ethanol ester of flufenamic acid. *US Patent* 4980498.

5. Almasirad, A., Tajik, M., Bakhtiari, D., Shafiee, A., Abdollahi, M., Zamani, M.J., Khorasani, R. & Esmaily, H. (2005). Synthesis and analgesic activity of N-arylhydrazone derivatives of mefenamic acid. *J. Pharm. Pharm. Sci.* 8, 419–425.

6. Somani, R.R. & Bhanushali, U.V. (2011). Synthesis and evaluation of the anti-inflammatory, analgesic and ulcerogenic potential of NSAIDs bearing 1, 3, 4-oxadiazole scaffold. *Indian J. Pharm. Sci.* 73, 634–640. DOI: 10.4103/0250-474X.100237.

7. Salih, N., Salimon, J., Hameed, A. & Yousif, E. (2011). Synthesis, characterization and antimicrobial evaluation of some 1,3,4-oxadiazole derivatives. *Int. J. Pharm. Tech. Res.* 3, 1097–1102.

8. Malhotra, M., Sanduja, M., Samad, A. & Deep, A. (2012). New oxadiazole derivatives of isonicotinohydrazide in the search for antimicrobial agents: synthesis and *in vitro* evaluation. *J. Serb. Chem. Soc.* 77, 9–16. DOI: 10.2298/JSC110123155M.

9. Singh, I. & Kumar, A. (2015). Synthesis and antibacterial activity of 2-(substituted phenyl)-5-(pyridin-4-yl)-1,3,4-oxadiazoles. *Chem. Sci. Trans.* 4, 133–136. DOI: 10.7598/cst2015.941.

10. Sahu, V.K.R., Singh, A.K. & Yadav, D. (20111). Review article on 1,3,4-oxadiazole derivatives and its pharmacological activities. *Int. J. Chem. Tech. Res.* 3, 1362–1372.

11. Husain, A. & Ajmal, M. (2009). Synthesis of novel 1, 3, 4-oxadiazole derivatives and their biological properties. *Acta Pharm.* 59, 223–233. DOI: 10.2478/v10007-009-0011-1.

12. Singh, A.K., Lohani, M. & Parthsarthy, R. (2013). Synthesis, characterization and anti-inflammatory activity of some 1,3,4-oxadiazole derivatives. *Iran J. Pharm. Res.* 12, 319–323.

13. Joshi, S.D., Vagdevi, H.M., Vaidya, V.P. & Gadaginamath, G.S. (2008). Synthesis of new 4-pyrrol-1-yl benzoic acid hydrazide analogs and some derived oxadiazole, triazole and pyrrole ring systems: A novel class of potential antibacterial and antitubercular agents. *Eur. J. Med. Chem.* 43, 1989–1996. DOI: 10.1016/j.ejmech.2007.11.016.

14. Redhu, S. & Kharb, R. (2013). Recent updates on chemistry and pharmacological aspects of 1, 3, 4-oxadiazole scaffold. *Int. J. Pharm. Innovation.* 3, 93–110.

15. de Oliveira, C.S., Lira, B.F., Barbosa-Filho, J.M., Lorenzo, J.G. & de Athayde-Filho, P.F. (2012). Synthetic approaches and pharmacological activity of 1,3,4-oxadiazoles: a review of the literature from 2000-2012. *Molecules.*17, 10192–10231. DOI: 10.3390/molecules170910192.

16. Bhat, K., Sufeera, K. & Chaitanya, S.K. (2011). Synthesis, characterization and biological activity studies of 1,3,4-oxadiazole analogs. *J. Young Pharm.* 3, 310–314. DOI: 10.4103/0975-1483.90243.

17. Azzawi, A.M.A. & Al-Obiadi, K.K.H. (2016). Synthesis and antimicrobial screening new bis Shiff bases and their acetyl oxadiazole azetidinone derivatives from pyromelliticdiimide. *Int. J. Res. Pharm. Chem.* 6, 1–8.

18. Yar, M.S., Siddiqui, A.A. & Ali, M.A. (2007). Synthesis and anti tuberculostatic activity of novel 1,3,4-Oxadiazole derivatives. *J. Chin. Chem. Soc.* 54, 5–8. DOI: 10.1002/JCCS.200700002.

19. Singh, R. & Chouhan, A. (2014). Various approaches for synthesis of 1, 3, 4-Oxadiazole derivatives and their pharmacological activity. *World J. Pharm. Pharm. Sci.* 3, 1474–1505.

20. Zheng, X., Li, Z., Wang, Y., Chen, W., Huang, Q., Liu, C. & Song, G. (2003). Syntheses and insecticidal activities of novel 2,5-disubstituted 1,3,4-oxadiazoles. *J. Fluorine Chem.* 123, 163–169. DOI: 10.1016/S0022-1139(03)00168-4.

21. Kumar, R., Yar, M.S., Rai, A.K. & Chaturvedi, S. (2013). Synthesis and biological evaluation of some novel 1, 3, 4-oxadiazoles derived from bi phenyl 4- carboxylic acid. *Der Pharm. Lett.* 5, 366–370.

22. Stanzione, F., Giangreco, I. & Cole, J. (2021). Use of molecular docking computational tools in drug discovery. *Prog. Med. Chem.* 60, 273–343. DOI: 10.1016/bs.pmch.2021.01.004.

23. Morris, G.M. & Lim-Wilby, M. (2008). Molecular docking. *Methods Mol. Biol.* 443, 365–382. DOI: 10.1007/978-1-59745-177-2_19.

24. Khalaf, H.S., Naglah, A.M., Al-Omar, M.A., Moustafa, G.O., Awad, H.M. & Bakheit, A.H. (2020). Synthesis, docking, computational studies, and antimicrobial evaluations of new dipeptide derivatives based on nicotinoylglycylglycine hydrazide. *Molecules*, 25, 3589. DOI: 10.3390/molecules25163589.

25. Silakari, O. & Singh, P.K. (2021). Chapter 14 – ADMET tools: Prediction and assessment of chemical ADMET properties of NCEs. *Concepts and Experimental Protocols of Modelling and Informatics in Drug Design*, 299–320. DOI: 10.1016/B978-0-12-820546-4.00014-3.

26. Halgren, T.A. (1996). Merck molecular force field. I. Basis, form, scope, parameterization, and performance of MMFF94. *J. Comput. Chem.* 17, 490–519. DOI: 10.1002/(SICI)1096-987X(199604)17:5/6<490::AID-JCC1>3.0.CO;2-P.

27. Dewar, M.J.S., Zoebisch, E.G., Healy, E.F. & Stewart J.J.P. (1985). Development and use of quantum mechanical molecular models. 76. AM1: a new general purpose quantum mechanical molecular model. *J. Am. Chem. Soc.* 107, 3902–3909. DOI: 10.1021/ja00299a024.

28. Chandrasekhar, T., Kumar, L.V., Reddy, A.B., Naik, J.P. & Swamy, G.N. (2012). Synthesis and biological evaluation of some new aryl acid N0 – (1Hindazole-3-carbonyl)-hydrazide derivatives. *J. Chem. Pharm. Res.* 4, 2795–2802.

29. Onnis, V., Cocco, M.T., Fadda, R. & Congiu, C. (2009). Synthesis and evaluation of anticancer activity of 2-arylamino-6-trifluoromethyl-3-(hydrazonocarbonyl)pyridines. *Bioorg. Med. Chem.* 17, 6158–6165. DOI: 10.1016/j.bmc.2009.07.066.

30. Reddy, L.V., Suman, A., Beevi, S.S., Mangamoori, L.N., Mukkanti, K. & Pal, S. (2010). Design and synthesis of 1-aroyl-2-ylidene hydrazines under conventional and microwave irradiation conditions and their cytotoxic activities. *J. Braz. Chem. Soc*. 21, 98–104. DOI: 10.1590/S0103-50532010000100015.

31. Bhat, M.A., Al-Omar, M.A., Alsaif, N.A., Almehizia, A.A., Naglah, A.M., Razak, S., Khan, A.A. & Ashraf, N.M. (2020). Novel sulindac derivatives: synthesis, characterisation, evaluation of antioxidant, analgesic, anti-inflammatory, ulcerogenic and COX-2 inhibition activity. *J. Enz. Inhib. Med. Chem.* 35, 921–934. DOI: 10.1080/14756366.2020.

32. Bhat, M.A. (2014). Synthesis and anti-mycobacterial activity of new 4-thiazolidinone and 1,3,4-oxadiazole derivatives of isoniazid. *Acta Pol. Pharm.* 71, 763–770.

33. Bhat, M.A., Khan, S.A. & Siddiqui, N. (2005). Synthesis and antibacterial activity of coumarin incorporated 1,3,4-oxadiazoles. *Indian J. Het. Chem.* 14, 271–272.